An Approximate Nonlinear Analysis of Tunnel-Diode Converters

CHARLES C. H. TANG

Abstract—Approximate analyses published previously[1]–[8] on tunnel-diode converters are basically phenomenological in nature by restricting the currents flowing through the tunnel diode or (and) the voltage across it to the signal, local oscillator, and intermediate frequencies only. Because of the nonlinear nature of the tunnel diode, many higher-order frequency components corresponding to harmonics and products, sums, and differences of the above mentioned frequencies are present. By including the effects of series resistance and series inductance and restricting the operating region within the parabolic portion of the tunnel-diode characteristics, the present analysis attempts to formulate the problem in a "rigorous" manner through the derivation of a second-order nonautonomous nonlinear differential equation with time-varying coefficients. The solution to a "first-order" approximation is obtained by incorporating a variational type treatment with an expansion type perturbation method.

In an effort to verify the validity of the theoretical results obtained by the nonlinear analysis, an analog simulation is carried out since the control of required parameters in actual experiments is extremely difficult, especially in the microwave frequency region. The general agreement between the theoretical results and the analog simulation is promising and, therefore, should yield enough information to facilitate the control and adjustment of the various parameters in actual experiments especially in the microwave region. Specifically, we have verified by the analog simulation the theoretical prediction that the optimized conversion gain is obtained when the source resistance is about one third of the load resistance.

In addition to minimizing the converter noise, the noise due to the first IF amplifier can also be minimized by selection of the correct converter load resistance by using Figs. 4 through 8.

Introduction

In most RF receivers, frequency down-converters or mixers precede high-amplification IF strips in order to facilitate amplification processes. Conventional crystal converters inevitably introduce conversion loss and therefore degrade the overall noise figure whereas a tunnel-diode converter can offer a low overall noise figure because of its conversion gain[1] and possible low excess noise power. The alternative method of using parameteric amplifiers at RF can offer comparable low overall noise figure but the need of an extra source at a pump frequency makes this scheme somewhat less attractive in comparison with tunnel-diode converters.

In earliest studies on tunnel-diode converters[1],[2] in the UHF region, the problem is simplified by assuming that the series resistance and series inductance of the tunnel diode are negligible in its equivalent circuit. In the microwave region[3] however, these series components may not be insignificant and should be included in the analysis. By restricting the operating region in that portion of the tunnel-diode characteristics which can be approximated by a parabola, we present a generalized analytic approach including the effects of the series resistance, series inductance, and time-varying shunt capacitance of a tunnel diode used as a down-converter at microwave frequencies.

Manuscript received January 30, 1967; revised May 24, 1967.

The author was with Bell Telephone Laboratories, Inc., Holmdel, N. J. He is currently with Bellcomm, Inc., Washington, D. C.

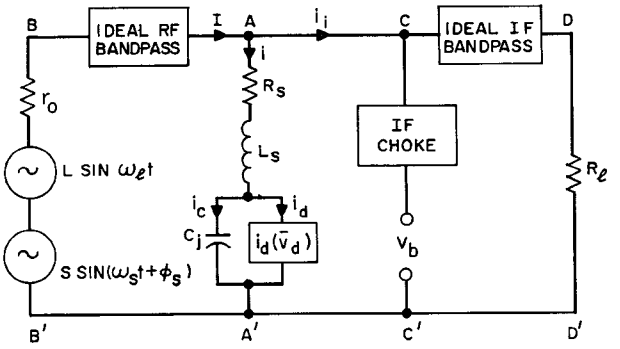

Fig. 1. A tunnel-diode converter circuit.

The complete circuit of a tunnel-diode down-converter is shown in Fig. 1. Across the tunnel diode, the RF branch $ABB'A'$ consists of a signal of an amplitude S, a local oscillator or pump of an amplitude L, an equivalent source resistance r_0, and an ideal RF bandpass filter; the biasing branch $ACC'A'$ consists of a dc bias voltage V_b and an IF choke; the IF branch $ADD'A'$ consists of a load resistance R_l, and an ideal IF transmission filter.

We stipulate that the bias condition for the tunnel diode operating as a converter be such that the average conductance be positive in order to prevent oscillation regardless of termination. This requires that the dc bias voltage V_b be less than the voltage v_p at the peak of the $\bar{v}$–i characteristic. If we further stipulate that the maximum LO excursion point is not allowed to reach near the inflection point p of the $\bar{v}$–i characteristic shown in Fig. 2, we can assume that the region of our interest in the $\bar{v}$–i characteristic of the tunnel diode can be represented very closely by a parabolic relation

$$i_d = a\bar{v}_d - b\bar{v}_d^2 = a\bar{v}_d\left(1 - \frac{\bar{v}_d}{2v_p}\right) = f(\bar{v}_d) \tag{1}$$

with

$$\bar{v}_d = v_d + V_b \tag{2}$$

where v_d is the "ac" voltage developed directly across the nonlinear resistance of the tunnel diode, and the constants a and b can be found by fitting the parabolic section of $\bar{v}$–i characteristic of the actual tunnel diode in question. Fig. 2 shows a typical germanium tunnel-diode characteristic and the idealized parabola.

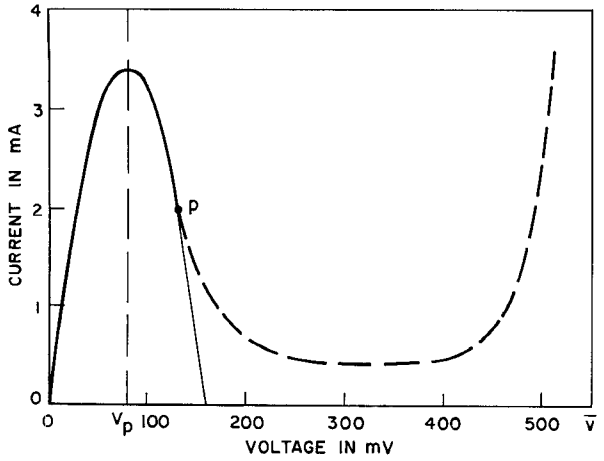

Fig. 2. $\bar{v}$–i characteristic of a tunnel diode.

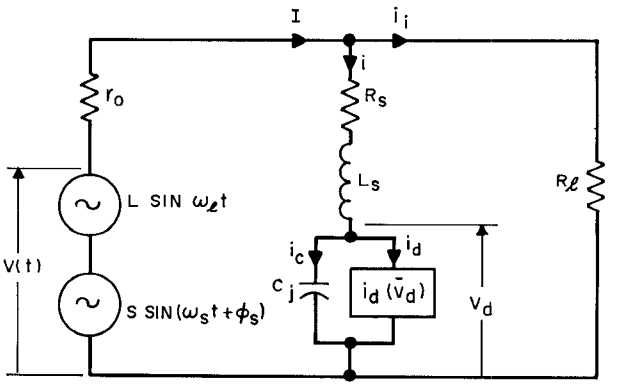

Fig. 3. A simplified tunnel-diode circuit.

Formulation

For purposes of analysis the circuit of Fig. 1 can be simplified as shown in Fig. 3. Because of the nonlinear nature of the tunnel diode, v_d may consist of voltages of many frequencies and we want to find v_d by deriving and solving the differential equation in v_d. The source resistance r_0 and the load resistance R_l are among the unknowns to be solved and should assume different apparent values for currents of different frequencies because of the actual presence of filtering circuits in different loops. This statement will be explained more explicitly later. Fig. 3 supplies the following general equations

$$v_d = V(t) - Ir_0 - iR_s - L_s\frac{di}{dt} \tag{3}$$

$$i = i_c + i_d = \frac{d}{dt}(C_j v_d) + f(\bar{v}_d) \tag{4}$$

$$I = i + i_i = i + \left(v_d + iR_s + L_s\frac{di}{dt}\right)\frac{1}{R_l}. \tag{5}$$

Combining (1) to (5), we have the differential equation

$$L_s C_j Q\frac{d^2v_d}{dt^2} + \left\{\left[\left(a - 2bV_b + 2\frac{dC_j}{dt}\right)L_sQ + C_jK\right] - 2bL_sQv_d\right\}\frac{dv_d}{dt} + \left[Q + K\left(a - 2bV_b + \frac{dC_j}{dt}\right) + L_sQ\frac{d^2C_j}{dt^2}\right]v_d - bKv_d^2 + (a - bV_b)V_bK = V(t) \tag{6}$$

where

$$Q = 1 + \frac{r_0}{R_l},$$

$$K = r_0 + R_s + \frac{r_0R_s}{R_l} \tag{7}$$

and

$$V(t) = L\sin\omega_l t + S\sin(\omega_s t + \phi_s). \tag{8}$$

Letting

$$A = \frac{K}{L_sQ} + \frac{a - 2bV_b}{C_j} + 2\frac{d}{dt}\log C_j,$$

$$B = \frac{2b}{C_j},$$

$$C = \frac{1}{L_sC_j}\left[1 + \frac{K}{Q}(a - 2bV_b)\right] + \frac{K}{L_sQ}\frac{d}{dt}\log C_j + \frac{1}{C_j}\frac{d^2C_j}{dt^2},$$

$$D = \frac{bK}{L_sC_jQ},$$

$$E = \frac{(a - bV_b)V_bK}{L_sC_jQ},$$

$$F = \frac{1}{L_sC_jQ}[L\sin\omega_l t + S\sin(\omega_s t + \phi_s)] \tag{9}$$

we have from (6)

$$\frac{d^2v_d}{dt^2} + Cv_d = F - E + Dv_d^2 - (A - Bv_d)\frac{dv_d}{dt}. \tag{10}$$

Clearly (10) is a second-order nonautonomous nonlinear differential equation with time-varying coefficients.

To estimate the effect of time-varying terms on the coefficients, we have to investigate how C_j varies with time. For a p–n junction the associated nonlinear capacitance C_j is a function of the applied voltage. Since we stipulate that the bias voltage V_b is less than the peak voltage v_p and the maximum LO excursion point does not reach the inflection point p, the variation of the capacitance ΔC is small in comparison with the capacitance C_{jb} at the bias voltage V_b. Therefore, the nonlinear capacitance is approximately equivalent to a time-varying capacitance[9]

$$C_j = C_{jb} + \Delta C\sin\omega_l t.$$

It follows that

$$\frac{d}{dt}\log C_j \doteq \omega_l \frac{\Delta C}{C_j}\cos \omega_l t$$

$$\frac{1}{C_j}\left(\frac{d^2C_j}{dt^2}\right) \doteq -\omega_l{}^2 \frac{\Delta C}{C_j}\sin \omega_l t.$$

It is obvious that as long as ω_l is not too high (i.e., $\omega_l < \omega_0$, where ω_0 is the natural frequency of the converter system, to be explained later) and ΔC is smaller than C_j, the time-varying terms can be neglected. By dropping the terms containing the time derivatives of C_j, the coefficients of (9) become

$$A = \frac{1}{L_s}\cdot\frac{K}{Q} + \frac{a - 2bV_b}{C_j},$$

$$B = \frac{2b}{C_j},$$

$$C = \frac{1}{L_sC_j}\left[1 + (a - 2bV_b)\frac{K}{Q}\right],$$

$$D = \frac{b}{L_sC_j}\cdot\frac{K}{Q},$$

$$E = \frac{(a - bV_b)V_b}{L_sC_j}\cdot\frac{K}{Q},$$

$$F(t) = \frac{1}{L_sC_jQ}[L\sin \omega_l t + S\sin(\omega_s t + \phi_s)]. \quad (11)$$

It is important to note that, except B and F, all coefficients are a function of K/Q, whereas F is a function of Q alone. This means that the effective magnitude of the forcing function F depends only on the actual value of $Q = 1 + r_0/R_l$.

If the following condition is fulfilled

$$C > Dv_d \quad (12)$$

and the terms $A(dv_d/dt)$ and $Bv_d(dv_d/dt)$ can be considered as small linear and nonlinear damping terms, respectively, we can now identify the square root of the coefficient C as the natural frequency ω_0 of the system. The term $[F(t) - E]$ is the forcing function. Note that the natural frequency ω_0 of the converter system is inversely proportional to the square root of L_sC_j and it becomes larger, or smaller, than $1/\sqrt{L_sC_j}$ depending on whether V_b is smaller, or larger, than the peak voltage v_p of the $\bar{v}$–i characteristic of the tunnel diode in question. In addition it is a function of R_s, r_0, and R_l and therefore it is considerably more sophisticated than the conventional expression

$$\omega_0 = \frac{1}{\sqrt{L_sC_j}}\sqrt{1 - \frac{L_s}{C_jR_e^2}}.$$

We now attempt to solve the nonautonomous nonlinear differential (10) to a first-order approximation by a method incorporating a variational treatment and an expansion-type perturbational treatment. If both L and S can be considered as "hard" forcing functions, we can write (10) in the parameter form

$$\frac{d^2v_d}{dt^2} + \omega_0{}^2v_d = \epsilon\left[Dv_d{}^2 - (A - Bv_d)\frac{dv_d}{dt}\right] + [L'\sin \omega_l t + S'\sin(\omega_s t + \phi_s) - E] \quad (13)$$

where ϵ is a small parameter to be used in an expansion and

$$L' = \frac{L}{L_sC_jQ},$$

$$S' = \frac{S}{L_sC_jQ}. \quad (14)$$

Before solving (13) we introduce

1) the following set of values for a typical germanium tunnel diode suitable for use as a down-converter:

$$a = 86 \times 10^{-3}\ \text{V},$$
$$b = 0.54 \times 10^{-3}\ \text{V/mV},$$
$$C_j = 1 \times 10^{-12}\ \text{F},$$
$$L_s = 0.3 \times 10^{-9}\ \text{H},$$
$$R_s = 2.5\ \Omega; \quad (15)$$

2) the following operating frequencies:

$$f_l = 4170\ \text{MHz},$$
$$f_s = 4100\ \text{MHz}; \quad (16)$$

3) the following range of operation for:

$$L = 60 - 90\ \text{mV},$$
$$S \ll L,$$
$$V_b = 55 - 75\ \text{mV}. \quad (17)$$

Values in (15) to (17) show that (12) can always be satisfied for a wide range of r_0 and R_l.

We shall assume a general perturbation solution of (13) in the form of an asymptotic series

$$v_d = v_0 + \epsilon v_1 + \epsilon^2 v_2 + \epsilon^3 v_3 + \cdots. \quad (18)$$

The solution (18) is expected to be quasi-harmonic and v_0 is the "zeroth-order" harmonic solution termed as the generating solution. It is evident that v_0 is the solution of (13) as ϵ approaches zero. Poincare[10] has shown that solution (18) is analytic in terms of its parameter ϵ. Writing (18) in terms of the generating solution, we have

$$v_d = G\sin(\omega_l t + \theta) + H\sin \omega_l t + T\sin(\omega_s t + \phi_s) + P + \epsilon v_1 + \epsilon^2 v_2 + \cdots \quad (19)$$

where

$$G = G(t),$$
$$\theta = \theta(t); \quad (20)$$

$$H = \frac{L'}{\omega_0{}^2 - \omega_l{}^2},$$

$$T = \frac{S'}{\omega_0{}^2 - \omega_s{}^2}; \quad (21)$$

$$P = -\frac{E}{\omega_0{}^2}. \quad (22)$$

In passing it is pointed out that both G and θ will be constants as ϵ approaches zero. The procedure now is to develop by iterative processes higher-order solutions with the aid of the small parameter ϵ. Considering only the first-order solution, we are led to the variational equations

$$\frac{d^2G}{dt^2} - 2G\omega_0\frac{d\theta}{dt} - G\left(\frac{d\theta}{dt}\right)^2 = \epsilon\left\{2DG[H\sin\omega_l t + T\sin(\omega_s t+\phi_s)+P] - A\frac{dG}{dt} + B\left[\frac{dG}{dt}(H\sin\omega_l t + T\sin(\omega_s t+\phi_s)+P) + \omega_l GH\cos\omega_l t + \omega_s GT\cos(\omega_s t+\phi_s)\right]\right\} \quad (23)$$

$$G\frac{d^2\theta}{dt^2} + 2\omega_0\frac{dG}{dt} + 2\frac{dG}{dt}\frac{d\theta}{dt} = \epsilon\left\{-AG\left(\omega_0+\frac{d\theta}{dt}\right) + BG\left(\omega_0+\frac{d\theta}{dt}\right)\cdot[H\sin\omega_l t + T\sin(\omega_s t+\phi_s)+P]\right\} \quad (24)$$

and the perturbation equation

$$\begin{aligned}\frac{d^2v_1}{dt^2} + \omega_0^2 v_1 &= \frac{D}{2}(H^2+T^2+2P^2) + \frac{G}{2}\left(DG + B\frac{dG}{dt}\right)\\ &+ H[2DP\sin\omega_l t + \omega_l(BP-A)\cos\omega_l t]\\ &+ T[2DP\sin(\omega_s t+\phi_s) + \omega_s(BP-A)\cos(\omega_s t+\phi_s)]\\ &+ \frac{H^2}{2}[B\omega_l\sin 2\omega_l t - D\cos 2\omega_l t]\\ &+ \frac{G}{2}\left[BG\left(\omega_0+\frac{d\theta}{dt}\right)\sin 2(\omega_0 t+\theta) - \left(DG + B\frac{dG}{dt}\right)\cos 2(\omega_0 t+\theta)\right]\\ &+ \frac{T^2}{2}[B\omega_s\sin 2(\omega_s t+\phi_s) - D\cos 2(\omega_s t+\phi)]\\ &+ HT\left\{\frac{B}{2}(\omega_l+\omega_s)\sin[(\omega_l+\omega_s)t+\phi_s] - D\cos[(\omega_l+\omega_s)t+\theta_s]\right\}\\ &+ HT\left\{D\cos[(\omega_l-\omega_s)t-\phi_s] - \frac{B}{2}(\omega_l-\omega_s)\sin[(\omega_l-\omega_s)t-\phi_s]\right\}. \end{aligned} \quad (25)$$

Assuming both G and θ are slowly varying functions of time, we can retain only the first-order terms in (23) and (24), respectively, as

$$\frac{d\theta}{dt} = -\frac{\epsilon}{2\omega_0}\{2D[H\sin\omega_l t + T\sin(\omega_s t+\phi_s)+P] + B[\omega_l H\cos\omega_l t + \omega_s T\cos(\omega_s t+\phi_s)]\} \quad (26)$$

$$\frac{dG}{dt} = \frac{\epsilon G}{2}\{-A + B[H\sin\omega_l t + T\sin(\omega_s t+\phi_s)+P]\}. \quad (27)$$

The solutions of (26) and (27) are, respectively,

$$\theta = -\frac{\epsilon}{2\omega_0}\left\{2D\left[Pt - \frac{H}{\omega_l}\cos\omega_l t - \frac{T}{\omega_s}\cos(\omega_s t-\theta)\right] + B[H\sin\omega_l t + T\sin(\omega_s t+\theta_s)]\right\} \quad (28)$$

and

$$G = \exp\left(\frac{\epsilon}{2}\left\{(BP-A)t - B\left[\frac{H}{\omega_l}\cos\omega_l t + \frac{T}{\omega_s}\cos(\omega_s t+\phi_s)\right]\right\}\right). \quad (29)$$

The amplitude function G is exponentially decaying or rising depending on the sign of $(BP\text{-}A)$. From (22) and the values of (15) to (17) we note both A and B are positive quantities but P is always a negative quantity for bias voltage V_b less than v_p. Accordingly G approaches zero as time elapses, i.e., there is no steady-state natural frequency oscillation in the system as specified by the values in the range of (15) to (17). The solution of (25) therefore is

$$\begin{aligned} v_1 &= \frac{D}{2\omega_0^2}(H^2+T^2+2P^2)\\ &+ \frac{H}{\omega_0^2-\omega_l^2}[2DP\sin\omega_l t + \omega_l(BP-A)\cos\omega_l t]\\ &+ \frac{T}{\omega_0^2-\omega_s^2}[2DP\sin(\omega_s t+\phi_s) + \omega_s(BP-A)\cos(\omega_s t+\phi_s)]\\ &+ \frac{H^2}{2(\omega_0^2-4\omega_l^2)}[B\omega_l\sin 2\omega_l t - D\cos 2\omega_l t]\\ &+ \frac{T^2}{2(\omega_0^2-4\omega_s^2)}[B\omega_s\sin 2(\omega_s t+\phi_s) - D\cos 2(\omega_s t+\phi_s)]\\ &+ \frac{HT}{\omega_0^2-(\omega_l+\omega_s)^2}\left\{-D\cos[(\omega_l+\omega_s)t+\phi_s] + \frac{B}{2}(\omega_l+\omega_s)\sin[(\omega_l+\omega_s)t+\phi_s]\right\}\\ &+ \frac{HT}{\omega_0^2-(\omega_l-\omega_s)^2}\left\{D\cos[(\omega_l-\omega_s)t-\phi_s] - \frac{B}{2}(\omega_l-\omega_s)\sin[(\omega_l-\omega_s)t-\phi_s]\right\}. \end{aligned} \quad (30)$$

The first-order solution of (13) therefore is

$$\begin{aligned} v_{d1} &= M\sin(\omega_l t+\xi_l) + N\sin(\omega_s t+\phi_s+\xi_s)\\ &+ U\cos(2\omega_l t+\xi_{2l}) + W\cos(2\omega_s t+2\phi_s+\xi_{2s})\\ &+ X\cos[(\omega_l+\omega_s)t+\phi_s+\xi_{l+s}]\\ &+ Y\cos[(\omega_l-\omega_s)t-\phi_s] + J \end{aligned} \quad (31)$$

where

$$M = H\left[\left(1+\epsilon D\frac{2P}{\omega_0^2-\omega_l^2}\right)^2+\frac{\epsilon^2\omega_l^2(BP-A)^2}{(\omega_0^2-\omega_l^2)^2}\right]^{1/2},$$

$$\xi_l = \tan^{-1}\frac{\epsilon\omega_l(BP-A)}{\omega_0^2-\omega_l^2+\epsilon 2DP},$$

$$N = T\left[\left(1+\epsilon D\frac{2P}{\omega_0^2-\omega_s^2}\right)^2+\frac{\epsilon^2\omega_s^2(BP-A)^2}{(\omega_0^2-\omega_s^2)^2}\right]^{1/2},$$

$$\xi_s = \tan^{-1}\frac{\epsilon\omega_s(BP-A)}{\omega_0^2-\omega_s^2+\epsilon 2DP},$$

$$U = \frac{\epsilon DH^2}{2(\omega_0^2-4\omega_l^2)}\left[1+\frac{B^2\omega_l^2}{D^2}\right]^{1/2},$$

$$\xi_{2l} = \tan^{-1}\frac{-B\omega_l}{-D},$$

$$W = \frac{\epsilon DT^2}{2(\omega_0^2-4\omega_s^2)}\left[1+\frac{B^2\omega_s^2}{D^2}\right]^{1/2},$$

$$\xi_{2s} = \tan^{-1}\frac{-B\omega_s}{-D},$$

$$X = \frac{\epsilon DHT}{\omega_0^2-(\omega_l+\omega_s)^2}\left[1+\frac{B^2}{4D^2}(\omega_l+\omega_s)^2\right]^{1/2},$$

$$\xi_{l+s} = \tan^{-1}\frac{-B(\omega_l+\omega_s)}{-2D},$$

$$Y = \frac{\epsilon DHT}{\omega_0^2-(\omega_l-\omega_s)^2},$$

$$J = P+\epsilon D\frac{1}{2\omega_0^2}(H^2+T^2+2P^2). \tag{32}$$

It is important to note that the image frequency ($2\omega_l-\omega_s$) component of voltage does not appear across the tunnel-diode terminal v_{d1} in the first-order solution.

Examination of equations (32) shows that these coefficients may blow up at their respective singularities. Physically these singularities mean that oscillations may occur when the natural frequency ω_0 of the system is equal to ω_l or ω_s or their harmonics. Using the values of (15) to (17), we obtain from (11) that the natural frequency f_0 of the system varies from 10 to 20 GHz depending on the magnitudes of the biasing voltage V_b (always less than v_p for our converter use), source resistance r_0 and load resistance R_l. Simple approximations from these coefficients are possible when f_0 is much larger, or smaller, than the operating frequency f. It is quite clear now that tunnel-diode down-converters with gain can be successfully operated in the UHF region ($f \ll f_0$) whereas in the microwave region instability in operation has been the main difficulty in experiments. If we operate at 4 GHz and assume $f_0=9$ or 10 GHz, instability might not occur. If, however, $f_0=8$ or 12 GHz, obviously instability conditions are satisfied. On the other hand, if f_0 is near 20 or 24 GHz, we might not have the instability conditions, since these fifth or sixth harmonics are higher-order terms in the small expansion parameter ϵ. It is now theoretically clear that for stable mixer operations, we should look for tunnel diodes with very low C_j and L_s so that f_0 is way above the operating frequency f. The best way to reduce L_s and C_j is to fabricate the tunnel diode directly across the walls of the waveguide of reduced height. In what follows we shall only investigate the $\omega^2 \ll \omega_0^2$ case.

We note from (31) that the voltage v_{d1} developed across the nonlinear part of the tunnel diode does contain an IF component of amplitude Y. Because of the different filtering circuits in different branches, this IF component of voltage is effective only in the IF branch $ADD'A'$. We also note that the ac voltage v_{d1} has an average dc component J and the total apparent or equivalent dc bias across the tunnel diode now is V_b+J instead of V_b.

Having obtained the ac voltage across the nonlinear resistance part of the tunnel diode, we are now in a position to determine all the current components of i flowing through the tunnel-diode branch between A and A' of Fig. 2. We have from (4) and (31)

$$\begin{aligned} i_c &= C_j\frac{d}{dt}v_{d1} \\ &= C_j\{\omega_l M\cos(\omega_l t+\xi_l)+\omega_s N\cos(\omega_s t+\phi_s+\xi_s) \\ &\quad -2\omega_l U\sin(2\omega_l t+\xi_{2l})-2\omega_s W\sin(2\omega_s t+2\phi_s+\xi_{2s}) \\ &\quad -(\omega_l+\omega_s)X\sin[(\omega_l+\omega_s)t+\phi_s\xi_{l+s}] \\ &\quad -(\omega_l-\omega_s)Y\sin[(\omega_l-\omega_s)t-\phi_s]\} \end{aligned} \tag{33}$$

and from (1), (2), and (31)

$$\begin{aligned} i_d &= [a-b(V_b+J)](V_b+J)+[a-2b(V_b+J)] \\ &\quad \cdot\{M\sin(\omega_l t+\xi_l)+N\sin(\omega_s t+\phi_s+\xi_s) \\ &\quad +U\cos(2\omega_l t+\xi_{2l})+W\cos[2(\omega_s t+\phi_s)+\xi_{2s}] \\ &\quad +X\cos[(\omega_l+\omega_s)t+\phi_s\xi_{l+s})] \\ &\quad +Y\cos[(\omega_l-\omega_s)t-\phi_s]\} \\ &\quad -b\{M\sin(\omega_l t+\xi_l)+N\cos(\omega_s+\phi_s+\xi_s) \\ &\quad +U\cos(2\omega_l+\xi_{2l})+W\cos[2(\omega_s t+\phi_s)+\xi_{2s}] \\ &\quad +X\cos[(\omega_l+\omega_s)t+\phi_s+\xi_{l+s}] \\ &\quad +Y\cos[(\omega_l\omega_s)t-\phi_s]\}^2. \end{aligned} \tag{34}$$

For clarity purposes all components of the current $i=i_c+i_d$ are listed in the Appendix and are arranged in increasing frequency order in spectral form.

Picking up only the IF terms, we have

$$\begin{aligned} i_i &= i_{ci}+i_{di} \\ &= -C_j(\omega_l-\omega_s)Y\sin[(\omega_l-\omega_s)t-\phi_s] \\ &\quad +[a-2b(V_b+J)]Y\cos[(\omega_l-\omega_s)t-\phi_s] \\ &\quad -bMN\cos[(\omega_l-\omega_s)t+\xi_l-\xi_s-\phi_s] \\ &\quad -bUX\cos[(\omega_l-\omega_s)t+\xi_{l2s}-\xi_{l+s}-\phi_s] \\ &\quad -bWX\cos[(\omega_l-\omega_s)t-\xi_{l2s}-\xi_{l+s}-\phi_s]. \end{aligned} \tag{35}$$

It is important to note that as long as C_j is small and the IF is not too high, the component of IF current due to C_j is always negligibly small (relatively). By comparison of the magnitudes of the terms in (35), we have, assuming $\omega_0^2 \gg \omega_l^2$ and neglecting term of ϵ^2,

$$\begin{aligned} i_i &= [a-2b(V_b+J)]Y\cos[(\omega_l-\omega_s)t-\phi_s] \\ &\quad -bMN\cos[(\omega_l-\omega_s)t+\xi_l-\xi_s-\phi_s)]. \end{aligned} \tag{36}$$

Since $\xi_l = \xi_s$ as seen from (32), (36) can be simplified as

$$i_i = \{[a - 2b(V_b + J)]Y - bMN\} \cdot \cos[(\omega_l - \omega_s)t - \phi_s]. \quad (37)$$

Substituting (32) into (37) under the assumption $\omega_0^2 \gg \omega_l^2$, we have to first-order terms in ϵ,

$$i_i = \left\{[a - 2b(V_b + J)]\frac{\epsilon DHT}{\omega_0^2} - bHT\left(1 + \epsilon D\frac{4P}{\omega_0^2}\right)\right\} \cdot \{\cos[(\omega_l - \omega_s)t - \phi_s]. \quad (38)$$

Rearranging (38) and using (21) and (22), we have, dropping ϵ, the following IF current flowing in the load resistance R_l.

$$i_i = -bHT\left\{1 - \frac{D}{b\omega_0^2}[a - 2b(V_b + 2P + J)]\right\} \cdot \cos[(\omega_l - \omega_s)t - \phi_s] = -\left(\frac{bLS}{Q^2}\right)\frac{\left[1 + 2b(2P + J)\frac{K}{Q}\right]}{\left[1 + (a - 2bV_b)\frac{K}{Q}\right]^3} \cdot \cos[(\omega_l - \omega_s)t - \phi_s] \quad (39)$$

where

$$P = -\frac{E}{\omega_0^2} = -\frac{(a - bV_b)V_b\frac{K}{Q}}{1 + (a - 2bV_b)\frac{K}{Q}} \quad (40)$$

$$J \doteq P + \frac{D}{2\omega_0^2}(H^2 + 2P^2) = P + \frac{\frac{b}{2}\frac{K}{Q}}{\left[1 + (a - 2bV_b)\frac{K}{Q}\right]} \cdot \left\{\frac{\left(\frac{L}{Q}\right)^2}{\left[1 + (a - 2bV_b)\frac{K}{Q}\right]^2} + 2P^2\right\} \quad (41)$$

and

$$\frac{K}{Q} = \frac{R_l(r_0 + R_s) + r_0R_s}{R_l + r_0}. \quad (42)$$

Since we are interested only in the IF component of the current, the value of the effective load seen by the IF circuit can be obtained by letting the source resistance $r_0 \to \infty$ in the expression of K/Q. This is physically reasonable because of the presence of the RF bandpass filter in the RF circuit branch. From (42) we have

$$\frac{K}{Q} \xrightarrow[r_0 \to \infty]{} R_l + R_s. \quad (43)$$

Accordingly the IF current in final form is

$$i_i = -\left[\frac{bLSR_l^2}{(R_l + r_0)^2}\right]\frac{[1 + 2b(2P + J)(R_l + R_s)]}{[1 + (a - 2bV_b)(R_l + R_s)]^3} \cdot \cos[(\omega_l - \omega_s)t - \phi_s] \quad (44)$$

where

$$P = -\frac{(a - bV_b)V_b(R_l + R_s)}{1 + (a - 2bV_b)(R_l + R_s)} \quad (45)$$

and

$$J = P + \frac{\frac{b}{2}(R_l + R_s)}{[1 + (a - 2bV_b)(R_l + R_s)]} \cdot \left\{\frac{\left(\frac{LR_l}{R_l + r_0}\right)^2}{[1 + (a - 2bV_b)(R_l + R_s)]^2} + 2P^2\right\}. \quad (46)$$

Inspection of (44) shows the important fact that the IF current is linearly proportional to the signal amplitude S as it should be.

We are now in a position to calculate the maximum possible transducer or conversion gain (or loss), which is defined below as the ratio of the power delivered to the load resistance to the available signal power (i.e., for a "conjugate match" at both the source and load terminals):

$$G(\text{or Loss}) = \frac{i_i^2R_l}{\frac{S^2}{4r_0}} = \frac{4i_i^2R_lr_0}{S^2} = 4R_lr_0\left[\frac{bLR_l^2}{(R_l + r_0)^2}\right]^2\frac{[1 + 2b(2P + J)(R_l + R_s)]^2}{[1 + (a - 2bV_b)(R_l + R_s)]^6}. \quad (47)$$

The conversion gain is independent of the signal level as it should be. Optimizing the conversion gain with respect to source resistance r_0, we obtain the *simple and important result*

$$r_0 = \tfrac{1}{3}R_l. \quad (48)$$

Substitution of (48) into (47), we have the conversion gain expression in a manageable form in parameters as

$$G(\text{or Loss}) = \left(\frac{3}{4}\right)^3(bLR_l)^2\frac{[1 + 2b(2P + J)(R_l + R_s)]^2}{[1 + (a - 2bV_b)(R_l + R_s)]^6}. \quad (49)$$

As R_l approaches zero or infinity the conversion gain G approaches zero as it should.

Results and Discussions

Optimization of the conversion gain G in (49) with respect to the load resistance R_l is obviously very desirable but impossible, since we have to solve for the multiple roots of a seventh degree polynomial with unknown parameters as coefficients. On the other hand, the optimization can be easily obtained for given parameters V_b and L by

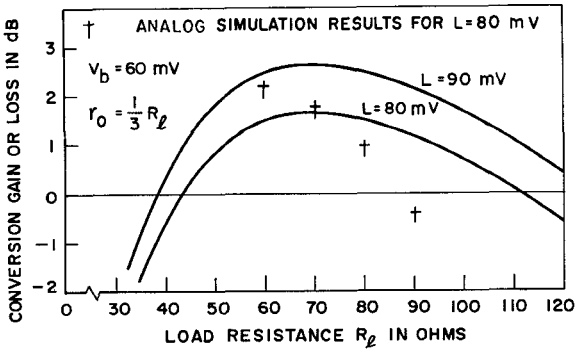

Fig. 4. Tunnel-diode converter characteristics.

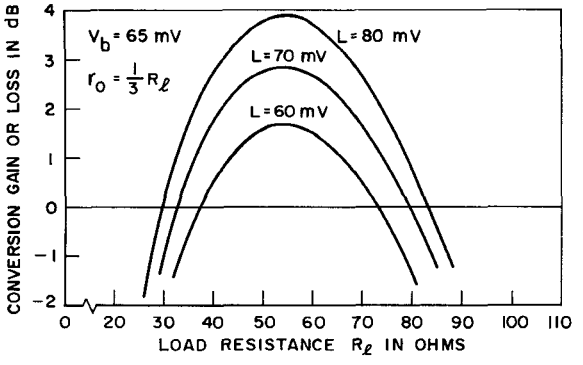

Fig. 5. Tunnel-diode converter characteristics.

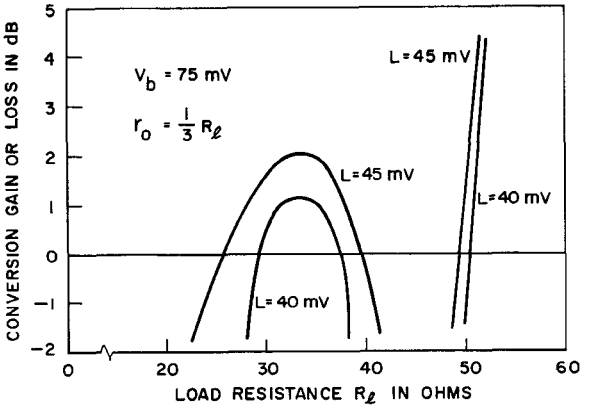

Fig. 6. Tunnel-diode converter characteristics.

using R_l as a variable to plot against G. This is carried out for various combinations of V_b and L in (49) and is shown in Figs. 4 through 6, for values of a, b, and R_s specified in (15). For completeness we also discuss the optimization of G with respect to V_b or L. Since at the start of the analysis we have restricted the ranges of V_b and L, respectively, any optimization with respect to these parameters does not mean too much for our purpose. Although these optimizations may give us arbitrary large conversion gain outside the specified range of V_b and L, our main interest lies in small conversion gain with stability which is only attainable experimentally or analogwise within the range of specified V_b and L for a parabolic $\bar{v}-i$ characteristic. It is seen from (49), that within the specified range of L, G

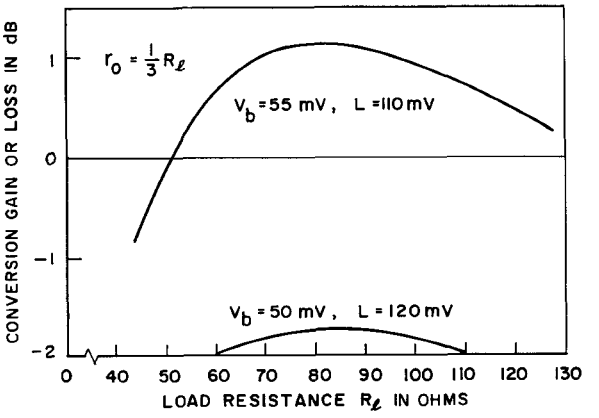

Fig. 7. Tunnel-diode converter characteristics.

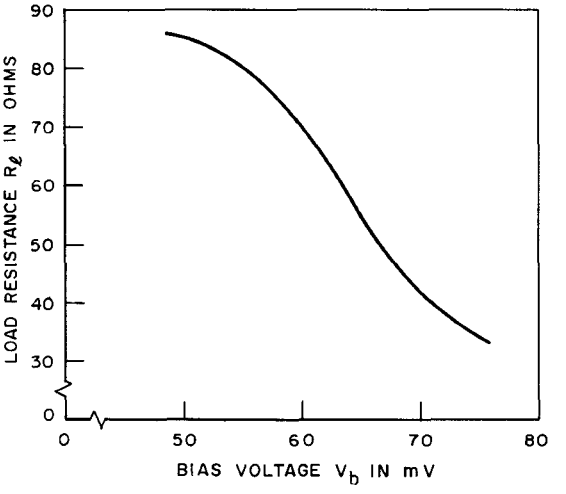

Fig. 8. V_b-R_l curve for optimized gain.

is only approximately proportional to the square of L since J is also a function of L. In general G increases rapidly with increasing bias voltage V_b and instability occurs with V_b approaching v_p. The combination choice of V_b and L must be such that the LO excursion point does not exceed the inflection point p. Figs. 4 through 7 show effects of V_b and L on G. It is seen that for a constant V_b the optimum load resistance R_l remains constant and independent of L. The optimum load resistance R_l for maximum conversion gain decreases with increasing V_b and is shown in Fig. 8 by cross plotting from Figs. 4 through 7. Finally we mention that G is approximately proportional to the square of b, the coefficient of the quadratic term of the parabolic $\bar{v}-i$ characteristic. Accordingly it is advantageous to choose a tunnel diode with $\bar{v}-i$ characteristic of large b and this, in turn, means those characteristics with steep slope and high peak current.

The choice of the magnitude of L to acquire a required conversion gain depends mainly on the choice of the bias voltage V_b. A smaller value of V_b always needs a larger value of L to obtain the prescribed gain as shown in Fig. 7. In order to have a conversion gain in this case, we have to use a value of L which is much larger than the specified range. From the point of view of reducing the shot noise in a tunnel-diode converter it is advisable to use relatively

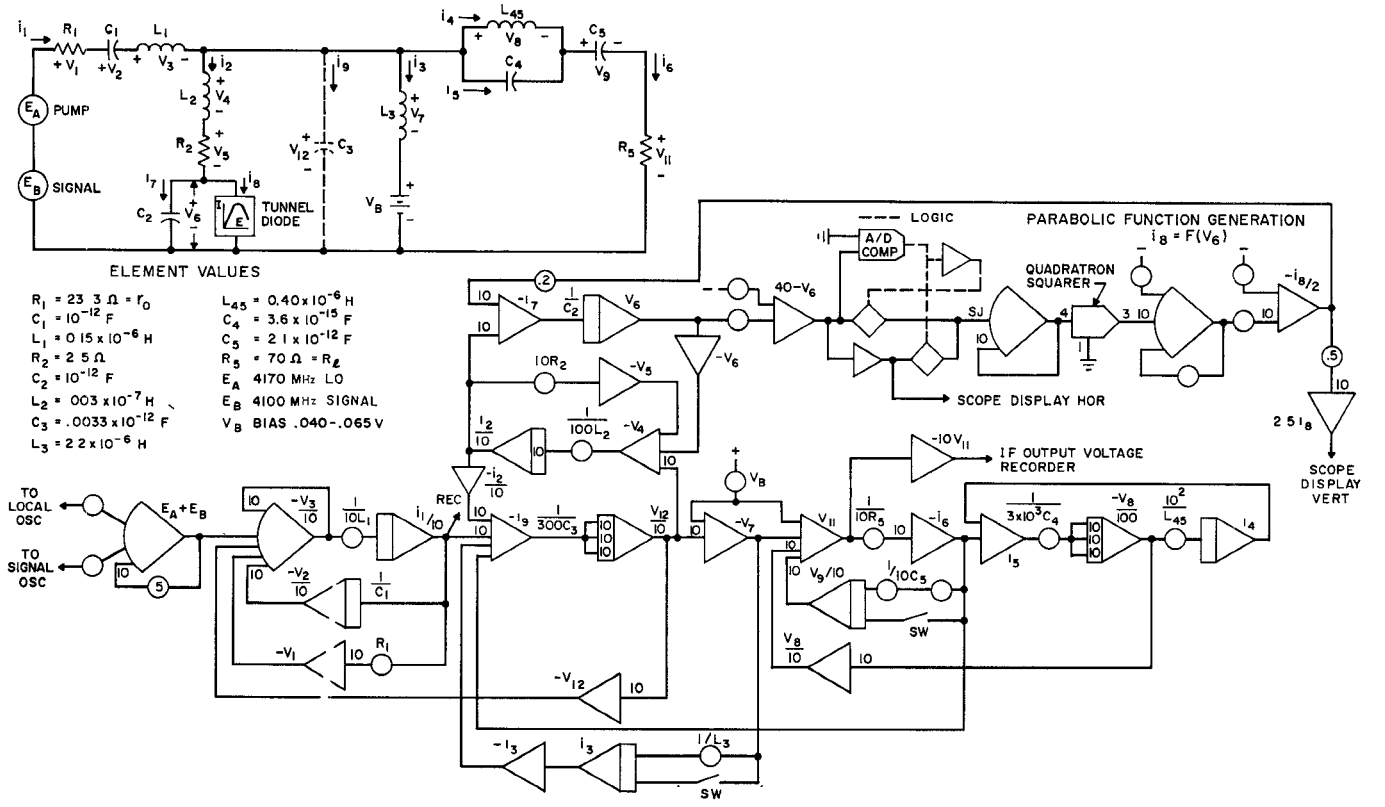

Fig. 9. Analog simulation circuit for tunnel-diode converters.

higher V_b and smaller L in such a way that the conversion gain remains small enough for stable operations. The combination of higher V_b and smaller L (Fig. 6) should limit the pumping excursion in a region where the shot noise is relatively small in comparison with that in the region near the origin where the shot noise is usually significantly enhanced. Because of the multiplicity of the roots usually there are several values of R_l which yield the same gain as shown in Fig. 6. The high gain region of R_l does not appear to have stable operation. The overall noise figure can be defined as[3]

$$F = \frac{N_0/S_0}{N_i/S_i} = 1 + \frac{N_e}{G_a N_a} \tag{50}$$

where

N_0 = actual noise power delivered at the output
S_0 = actual signal power delivered at the output
N_i = actual noise power delivered to the input
S_i = actual signal power delivered to the input
G_a = available power gain
N_e = excess noise power delivered at the output due to internal sources in the network
$N_a = kT\Delta f$ = available input noise power.

The overall noise figure of receiver can be improved by employing a tunnel-diode down-converter because of its conversion gain and possible low excess noise power according to (50).

We shall now turn to the results of the analog simulation. A block diagram of the analog circuit is shown in Fig. 9. The analog simulation has verified the theoretical prediction that when the source resistance r_0 is about one third of the load resistance R_l, the conversion gain is maximum. The conversion gain or loss, obtained from the analog simulation, is shown by daggers in Fig. 4 for the case of $L = 80$ mV and $V_b = 60$ mV. The simulation conversion gain or loss is computed from the ratio equivalent to (47), i.e.,

$$\begin{aligned} G \text{ (or Loss)} &= \left(\frac{V_l^2}{R_l}\right) \Big/ \left(\frac{S^2}{4r_0}\right) \\ &= \left(\frac{V_l^2}{R_l}\right) \Big/ \left(\frac{S^2}{4R_l/3}\right) \\ &= \frac{4}{3}\left(\frac{V_l}{S}\right)^2 \end{aligned} \tag{51}$$

where V_l is the IF voltage across the load resistance R_l.

The general agreement between the digital and analog results is both satisfying and promising and therefore should yield enough information to facilitate the control and adjustment of the various parameters in actual experiments, especially in the microwave region.

Appendix

Tunnel-Diode Components of the Current $i = i_c + i_d$

dc

$$[a - b(V_b + J)](V_b + J) - \frac{b}{2}\left[M^2 + N^2 + U^2 + W^2 + X^2 + Y^2\right]$$

$$
\begin{aligned}
\omega_l - \omega_s \quad & - bMN \cos [(\omega_l - \omega_s)t + \xi_l - \phi_s - \xi_s] \\
& - bUX \cos [(\omega_l - \omega_s)t + \xi_{2l} - \phi_s + \xi_{l+s}] \\
& - bWX \cos [(\omega_l - \omega_s)t - \phi_s - \xi_{2s} - \xi_{l+s}] \\
& + CY \cos [(\omega_l - \omega_s)t - \phi_s] \\
& - C_j(\omega_l - \omega_s) Y \sin [(\omega_l - \omega_s)t - \phi_s] \\
2(\omega_l - \omega_s) \quad & - bUW \cos [2(\omega_l - \omega_s)t + \xi_{2l} - 2\phi_s - \xi_{2s}] \\
& - bY^2 \cos [2(\omega_l - \omega_s)t - 2\phi_s]
\end{aligned}
$$

$$
\begin{aligned}
2\omega_s - \omega_l \quad & bMW \sin [(2\omega_s - \omega_l)t - \xi_l + 2\phi_s - \xi_{2s}] \\
& - bNY \sin [(2\omega_s - \omega_l)t + 2\phi_s + \xi_s] \\
\omega_s \quad & bMX \sin [\omega_s t - \xi_l + \phi_s + \xi_{l+s}] \\
& - bMY \sin (\omega_s t + \xi_l + \phi_s) \\
& + bNW \sin (\omega_s t + \phi_s - \xi_s + \xi_{2l}) \\
& + CN \sin (\omega_s t + \phi_s + \xi_s) \\
& + C_j\omega_s N \cos (\omega_s t + \phi_s + \xi_s) \\
\omega_l \quad & bMU \sin (\omega_l t - \xi_l + \xi_{2l}) \\
& - bNX \sin (\omega_l t + \xi_s - \xi_{l+s}) \\
& - bNY \sin (\omega_l t + \xi_s) \\
& + CM \sin (\omega_l t + \xi_l) C_j\omega_l M \cos (\omega_l t + \xi_l) \\
2\omega_l - \omega_s \quad & - bMY \sin [(2\omega_l - \omega_s)t + \xi_l - \phi_s] \\
& + bNU \sin [(2\omega_l - \omega_s)t - \phi_s - \xi_s + \xi_{2l}]
\end{aligned}
$$

$$
\begin{aligned}
3\omega_s - \omega_l \quad & - bWY \cos [(3\omega_s - \omega_l)t + 3\phi_s + \xi_{2s}] \\
2\omega_s \quad & - bXY \cos (2\omega_s t + 2\phi_s + \xi_{l+s}) \\
& + CW \cos (2\omega_s t + 2\phi_s + \xi_{2s}) \\
& + bN^2 \cos (2\omega_s t + 2\phi_s + 2\xi_s) \\
& + 2C_j\omega_s W \sin (2\omega_s t + 2\phi_s + \xi_{2s}) \\
\omega_l + \omega_s \quad & bMN \cos [(\omega_l + \omega_s)t + \xi_l + \phi_s + \xi_s] \\
& - bUY \cos [(\omega_l + \omega_s)t + \xi_{2l} + \phi_s] \\
& - bWY \cos [(\omega_l + \omega_s)t + \phi_s + \xi_{2s}] \\
& + CX \cos [(\omega_l + \omega_s)t + \phi_s + \xi_{l+s}] \\
& - C_j(\omega_l + \omega_s) X \sin [(\omega_l + \omega_s)t + \phi_s + \xi_{l+s}] \\
2\omega_l \quad & - bXY \cos (2\omega_l t + \xi_{l+s}) \\
& + CU \cos (2\omega_l t + \xi_{2l}) \\
& + bM^2 \cos (2\omega_l t + 2\xi_l) \\
& - 2C_j\omega_l U \sin (2\omega_l t + \xi_{2l}) \\
3\omega_l - \omega_s \quad & - bUY \cos [(3\omega_l - \omega_s)t + \xi_{2l} - \phi_s]
\end{aligned}
$$

$$
\begin{aligned}
3\omega_s \quad & - bNW \sin (3\omega_s t + 3\phi_s + \xi_s - \xi_{2l}) \\
2\omega_s + \omega_l \quad & - bMW \sin [(2\omega_s + \omega_l)t + \xi_l + 2\phi_s + \xi_{2s}] \\
& - bNX \sin [(2\omega_s + \omega_l)t + 2\phi_s + \xi_s + \xi_{l+s}] \\
2\omega_l + \omega_s \quad & - bMX \sin [(2\omega_l + \omega_s)t + \xi_l + \phi_s + \xi_{l+s}] \\
& - bNU \sin [(2\omega_l + \omega_s)t + \phi_s + \xi_s + \xi_{2l}] \\
3\omega_l \quad & - bMU \sin (3\omega_l + \xi_l + \xi_{2l})
\end{aligned}
$$

$$
\begin{aligned}
4\omega_s \quad & - bW^2 \cos (4\omega_s t + 4\phi_s + 2\xi_s) \\
3\omega_s + \omega_l \quad & - bWX \cos [(3\omega_s + \omega_l)t + 3\phi_s + \xi_{2s} + \xi_{l+s}] \\
2(\omega_l + \omega_s) \quad & - bUW \cos [2(\omega_l + \omega_s)t + \xi_{2l} + 2\phi_s + \xi_{2s}] \\
& - bX^2 \cos [2(\omega_l + \omega_s)t + 2\phi_s + 2\xi_{2s}] \\
3\omega_l + \omega_s \quad & - bUX \cos [(3\omega_l + \omega_s)t + \xi_{2l} + \phi_s + \xi_{l+s}] \\
4\omega_l \quad & - bU^2 \cos (4\omega_l t + 2\xi_{2l})
\end{aligned}
$$

where $C = a - 2b(V_b + J)$.

Acknowledgment

The author wishes to thank H. C. Rorden for the simulation results and Mrs. M. A. Styczynski for the digital computations.

References

[1] K. K. N. Chang, G. H. Heilmeier, and H. J. Prager, "Low-noise tunnel-diode down converter having conversion gain," *Proc. IRE*, vol. 48, pp. 854–858, May 1960.

[2] F. Sterzer and A. Presser, "Stable low-noise tunnel-diode frequency converter," *Proc. IRE (Correspondence)*, vol. 49, p. 1318, August 1961.

[3] C. S. Kim, "Tunnel-diode converter analysis," *IRE Trans. Electron Devices*, vol. ED-8, pp. 394–405, September 1961.

[4] R. A. Pucel, "Theory of the Esaki diode frequency converter," *Solid State Electronics*, vol. 3, pp. 167–207, November 1961.

[5] L. K. Nikulira, N. Y. Selivanenko, and V. S. Etkin, "Tunnel diode microwave frequency converters," *Telecommun. and Radio Engrg.*, pt. 1, vol, 18, pp. 1–11, September 1963.

[6] B. R. Davis, "A high frequency converter using tunnel diodes," *Proc. IRE* (Australia), vol. 25, pp. 25–32, January 1964.

[7] W. A. Gambling and S. B. Mallick, "Tunnel diode mixers," *Proc. IEE* (London), vol. 112, July 1965.

[8] M. R. Barber, "A numerical analysis of the tunnel-diode frequency converter," *IEEE Trans. Microwave Theory and Techniques*, vol. MTT-13, pp. 663–670, September 1965.

[9] W. H. Louisell, *Coupled Modes and Parametric Electronics*. New York: Wiley, 1960, p. 109.

[10] N. Minorsky, *Nonlinear Oscillations*. Princeton, N. J.: Van Nostrand, 1962, p. 215.